Beyond the Tavis-Cummings model: Revisiting cavity QED with ensembles of quantum emitters

Martin Blaha,[1,*] Aisling Johnson,[2,†] Arno Rauschenbeutel,[1] and Jürgen Volz[1,‡]
[1]*Department of Physics, Humboldt-Universität zu Berlin, 12489 Berlin, Germany*
[2]*Vienna Center for Quantum Science and Technology, Atominstitut, Technische Universität Wien, 1020 Vienna, Austria*

(Received 6 September 2021; accepted 7 December 2021; published 28 January 2022)

The interaction of an ensemble of N two-level quantum emitters with a single-mode electromagnetic field is described by the Tavis-Cummings model. There, the collectively enhanced light-matter coupling strength is given by $g_N = \sqrt{N}\bar{g}_1$, where $\bar{g}_1$ is the ensemble-averaged single-emitter coupling strength. This model has been employed to describe and to analyze numerous cavity-based experiments. Here, we show that this is only justified if the effective scattering rate into noncavity modes is negligible compared to the cavity's free-spectral range. In terms of experimental parameters, this requires that the optical depth of the ensemble is low, a condition that is violated in several state-of-the-art experiments. We give quantitative conditions for the validity of the Tavis-Cummings model and derive a more general Hamiltonian description that takes into account the cascaded interaction of the photons with all consecutive emitters. We show that the predictions of our cascaded model can differ quantitatively and even qualitatively from those obtained with the Tavis-Cummings model. Finally, we present experimental data, for which the deviation from the predictions of the Tavis-Cummings model is apparent. Our findings are relevant for all experiments in which optically dense ensembles of quantum emitters are coupled to an optical resonator.

DOI: 10.1103/PhysRevA.105.013719

I. INTRODUCTION

When strongly coupling a quantum emitter to a high-finesse optical resonator, one can control light-matter interaction at the fundamental level of individual photons. Such coupled emitter-resonator systems have proven successful for studying and harvesting cavity quantum electrodynamics (cQED) effects, ranging from the implementation of textbook models [1,2] to quantum-enhanced protocols with potential applications in quantum technology [3]. Recently, an increasing number of experiments go beyond cQED with single emitters and make use of the collective interaction of an ensemble of, e.g., atoms with the resonator mode to study complex many-body problems [4]. These experiments encompass cold atomic clouds [5–7] or Bose-Einstein condensates [8–11] that are coupled to one or several resonator modes with the aim of exploring phase transitions or novel regimes of cQED such as superstrong coupling [6,12]. The interaction of atomic ensembles with optical cavities has furthermore been proposed for metrology applications [5] or, in an integrated on-chip configuration, as a platform for quantum information processing [13,14]. A common aspect of many of these experiments is the realization of a large light-matter coupling strength based on the coherently enhanced collective interaction of many emitters with the cavity field. According to the Tavis-Cummings model [15,16], which we briefly recall in Sec. II below, the dynamics of the coupled system in the low excitation regime is identical to single-emitter cQED [17] but with a coupling strength $g_N = \sqrt{N}\bar{g}_1$ [15,16], where N is the number of emitters that collectively interact with the resonator mode and $\bar{g}_1$ is the ensemble-averaged single emitter-resonator coupling strength. Here, we study the limits of this approach and show that the standard Tavis-Cummings model breaks down for larger numbers of emitters (Sec. III) under conditions reached in many experiments. In order to go beyond the Tavis-Cummings model, we develop a real-space description of the coupled system (Sec. IV) that considers the successive interaction of N two-level quantum emitters with the propagating cavity field. We formulate a general Hamiltonian (Sec. VI), which is valid in a larger parameter range than the Tavis-Cummings model. We then derive an analytical solution for the stationary state of an ensemble of quantum emitters interacting with the modes of a ring resonator (Sec. VII) and compare the predictions of our cascaded model to the Tavis-Cummings model as well as to a generalization of the Tavis-Cummings model that accounts for more than one cavity mode (Sec. VIII). Finally, in Sec. IX, we apply the cascaded model to an experiment for which deviations from the Tavis-Cummings predictions are expected. We show that the cascaded model correctly describes the experiment where an ensemble of atoms is "superstrongly" coupled [12] to a 30-m-long ring resonator.

II. THE TAVIS-CUMMINGS MODEL

In the framework of the rotating wave approximation, the interaction of a single two-level quantum emitter, e.g., a single

*martin.blaha@hu-berlin.de
†Present address: Vienna Center for Quantum Science and Technology, Faculty of Physics, University of Vienna, 1090 Vienna, Austria.
‡juergen.volz@hu-berlin.de

atom, with a single electromagnetic field mode is described by the Jaynes-Cummings (JC) model [17]. The Hamiltonian reads

$$\frac{\hat{H}_{\mathrm{JC}}}{\hbar} = \omega_a \hat{\sigma}^+ \hat{\sigma}^- + \omega_c \hat{a}^\dagger \hat{a} + g_1(\hat{a}^\dagger \hat{\sigma}^- + \hat{a}\hat{\sigma}^+). \quad (1)$$

Here, $\hat{\sigma}^+$ ($\hat{\sigma}^-$) denotes the atomic raising (lowering) operator and $\hat{a}^\dagger$ ($\hat{a}$) is the photon creation (annihilation) operator. ω_a and ω_c are the atomic and cavity resonance frequencies, respectively, and g_1 is the single atom–single photon coupling strength which, without loss of generality, we assume to be real and positive.

Within the single excitation manifold of the {atom + cavity} system, the coupling of the atom to the resonator results in two new eigenstates with eigenenergies

$$E_{\mathrm{JC}} = \hbar\omega_c - \frac{\hbar}{2}\left(\Delta_{ca} \pm \sqrt{4g_1^2 + \Delta_{ca}^2}\right), \quad (2)$$

where $\Delta_{ca} = \omega_c - \omega_a$ is the cavity-atom detuning. For $\Delta_{ca} = 0$, this leads to the vacuum Rabi splitting of the unperturbed resonance into two split resonances separated in frequency by $2g_1$.

When describing an experimental {emitter + cavity} system, we have to account for losses. Two loss channels are typically considered: the spontaneous emission rate of the emitter into all free-space modes, γ_l, and the cavities field decay rate, κ_0, quantifying intracavity losses. These loss rates can be taken into account by introducing complex emitter and cavity resonance frequencies $\tilde{\omega}_a = (\omega_a - i\gamma_l)$ and $\tilde{\omega}_c = (\omega_c - i\kappa_0)$, respectively. For coupling the {emitter + cavity} system with an external probe field, the Hamiltonian has to be extended by the operator $\hat{U}_{\mathrm{probe}}$ which, e.g., for the case of a coherent probe field can be described as $\hat{U}_{\mathrm{probe}} = i\sqrt{2\kappa_{\mathrm{ext}}}\eta(\hat{a}^\dagger + \hat{a})$, where κ_{ext} is the coupling strength between the fields in and outside of the cavity and η is the amplitude of the probe field. Note that for the calculation in this paper we use the more general operator $\hat{U}_{\mathrm{probe}}$ in Appendix A. The resulting Hamiltonian, which now includes loss rates and probing, is given by

$$\frac{\hat{H}_{\mathrm{JC}'}}{\hbar} = \tilde{\omega}_a \hat{\sigma}^+ \hat{\sigma}^- + \tilde{\omega}_c \hat{a}^\dagger \hat{a} + g_1(\hat{a}^\dagger \hat{\sigma}^- + \hat{a}\hat{\sigma}^+) + \hat{U}_{\mathrm{probe}}. \quad (3)$$

A key figure that quantifies the performance of such an quantum emitter-resonator system is the so-called cooperativity of the coupled system

$$C = \frac{g_1^2}{2\kappa_0\gamma_l}, \quad (4)$$

where most experiments and applications aim for the regime $C \gg 1$. In this regime, the coupled system operates closely to the ideal, lossless system.

If more than one emitter is coupled to the resonator mode, the Jaynes-Cummings description has to be extended, yielding the Tavis-Cummings (TC) model [15]. Restricting the Hilbert space of the emitters to the subspace spanned by the fully symmetric Dicke states, and considering at most one excitation in the system, the collective ensemble excitation and annihilation operators are

$$\hat{S}^+ = \frac{1}{\sqrt{N}}\sum_{n=1}^{N}\hat{\sigma}_n^+ \quad \text{and} \quad \hat{S}^- = \frac{1}{\sqrt{N}}\sum_{n=1}^{N}\hat{\sigma}_n^-. \quad (5)$$

Using these operators, the TC Hamiltonian in the low excitation limit reads

$$\frac{\hat{H}_{\mathrm{TC}}}{\hbar} = \omega_a \hat{S}^+ \hat{S}^- + \omega_c \hat{a}^\dagger \hat{a} + g_N(\hat{a}^\dagger \hat{S}^- + \hat{a}\hat{S}^+). \quad (6)$$

A Hamiltonian describing the probed and lossy system can then be defined analogously to Eq. (3). From Eq. (6), it becomes apparent that the interaction between the ensemble and the resonator mode is formally the same as for a single emitter, but with a collectively increased coupling strength, $g_N = \sqrt{N}g_1$. The N emitters thus collectively behave as a "superatom" with a $\sqrt{N}$-fold increased coupling strength, thereby providing a straightforward strategy for enhancing light-matter coupling in experiments. Note that each emitter coupled to the resonator mode can in principle have a different coupling strength, $g_{1,n}$, e.g., due to the spatial variation of the cavity field. In this case, the Tavis-Cummings Hamiltonian Eq. (6) still applies when defining the collective coupling strength as

$$g_N = \left(\sum_{n=1}^{N} g_{1,n}^2\right)^{1/2} \equiv \sqrt{N}\bar{g}_1, \quad (7)$$

where $\bar{g}_1 = (\sum g_{1,n}^2/N)^{1/2}$ is the root mean square of the individual single-emitter coupling strengths.

III. LIMITS OF THE JAYNES-CUMMINGS AND THE TAVIS-CUMMINGS MODELS

We now discuss the conditions under which the Jaynes-Cummings and the Tavis-Cummings approaches are valid. An implicit assumption in the above models is that all relevant rates and frequency scales are small compared to the free spectral range ν_{FSR} (i.e., the inverse of the photon round trip time) of the resonator. However, two quantities can potentially violate this condition when the number of emitters N increases: the collective coupling strength, g_N, and the emitter-induced photon loss rate of the system, g_N^2/γ_l; see Appendix A. The JC or TC Hamiltonian is therefore only a valid description of the system if the inequalities

$$\nu_{\mathrm{FSR}} \gg g_N, \quad (8)$$

$$\nu_{\mathrm{FSR}} \gg \frac{g_N^2}{\gamma_l}, \quad (9)$$

are fulfilled. Violating condition (8) implies that the collective coupling strength reaches or exceeds the free spectral range of the resonator, thereby entering the so-called superstrong coupling regime of cQED [6,12]. This condition will typically only break down in experiments that were designed to explore this regime. Furthermore, the superstrong coupling regime can straightforwardly be included in the above description by considering the coupling of the quantum emitters to many cavity modes. In doing so, one obtains the multimode Tavis-

TABLE I. A list of experiments that violate conditions 8 or 9, and thus operate in a regime where deviations from the TC model can be observed. The violation ($g_N/\nu_{FSR} > 1$ and/or $g_N^2/(\gamma_l \nu_{FSR}) > 1$) is highlighted with bold numbers. Note that for the last column, we assumed no collectively enhanced emission of the ensemble into free space.

Reference	g_N	$\gamma_l \approx \gamma$	ν_{FSR}	g_N/ν_{FSR}	$g_N^2/(\gamma_l \nu_{\mathrm{FSR}})$
Lee *et al.* [18]	$2\pi \times 44.9$ MHz	$2\pi \times 3$ MHz	1.4 GHz	0.2	**3**
Johnson *et al.* [6]	$2\pi \times 9.2$ MHz	$2\pi \times 2.61$ MHz	7.1 MHz	**8.1**	**29**
Brennecke *et al.* [8]	$2\pi \times 3.5$ GHz	$2\pi \times 3$ MHz	850 GHz	0.026	**30**
Vaidya *et al.* [10]	$2\pi \times 464.9$ MHz	$2\pi \times 3$ MHz	15 GHz	0.195	**30**
Jiang *et al.* [19]	$2\pi \times 313$ MHz	$2\pi \times 2.87$ MHz	5.3 GHz	0.374	**41**
Colombe *et al.* [9]	$2\pi \times 12$ GHz	$2\pi \times 3$ MHz	3.9 THz	0.019	**77**

Cummings Hamiltonian, which reads

$$\frac{\hat{H}_{\mathrm{TCmm}}}{\hbar} = \omega_a \hat{S}^+ \hat{S}^- + \sum_j [\omega_j \hat{a}_j^\dagger \hat{a}_j + g_{N,j}(\hat{a}_j^\dagger \hat{S}^- + \hat{a}_j \hat{S}^+)], \tag{10}$$

where $\hat{a}_j^\dagger$ ($\hat{a}_j$) creates (annihilates) a photon in the jth mode of the resonator with frequency ω_j and $g_{N,j}$ is the coupling strength between the emitter and resonator mode j.

More importantly, condition (9) is more frequently violated in experiments, as is apparent from Table I, where we compare the parameters of different cQED experiments. Contrary to condition (8), the JC or TC model cannot be extended to account for the violation of (9), because when g_N^2/γ_l exceeds the free spectral range, the emitter-field interaction can no longer be treated as instantaneous. Consequently, one requires a description which considers the successive interaction of the field with each emitter. In the following, we will establish a model that is based on this approach.

IV. CAVITY AND WAVEGUIDE QED

At first, we will introduce typical waveguide QED parameters and relate them to the cQED quantities used in Sec. II. For this, we consider a quantum emitter coupled to a propagating optical mode, as sketched in Fig. 1. The emitter-mode coupling strength for this configuration is typically characterized by the β factor, defined as the ratio of the spontaneous emission rate of the emitter into the propagating mode, γ_{mode}, and the emission rate into all modes, $\gamma = \gamma_l + \gamma_{\mathrm{mode}}$. In general, as has recently been demonstrated [20], this emitter-mode coupling is not necessarily symmetric with respect to the forward and backward propagating modes. Therefore, two coupling constants must be introduced, denoted as β_+ for the forward and β_- for the backward propagating modes, with $\beta \equiv \beta_+ + \beta_-$. If the waveguide is now transformed into a Fabry-Pérot or ring resonator with a free spectral range ν_{FSR} (either by terminating the waveguide with mirrors or by closing the waveguide to form a ring), the vacuum Rabi frequency of the coupled emitter-resonator system is given by (see Appendix C)

$$g_1^2 = 4\beta\gamma\nu_{\mathrm{FSR}} \tag{11}$$

for a Fabry-Pérot cavity with the emitter placed at the antinodes of the standing wave in the cavity, and by

$$g_1^2 = 2\beta\gamma\nu_{\mathrm{FSR}} \tag{12}$$

for an emitter that is chirally coupled to a ring resonator. These equations give a direct relationship between characteristic cQED and waveguide QED parameters and illustrate that the emitter-resonator coupling strength is given by the geometric mean of the decay rate into the resonator mode, $\beta\gamma$, and the free spectral range, ν_{FSR}. From this, we also obtain the largest possible single emitter-resonator coupling strength for a given resonator length $g_{\max} = 2\sqrt{\gamma\nu_{\mathrm{FSR}}}$. Interestingly, for a given free spectral range, this maximum coupling strength is limited even though the cooperativity of the system approaches infinity for a perfectly coupled emitter, i.e., $\gamma_l \to 0$. We note that for free-space cavities, one can only approach this upper limit by employing cavity mirrors that cover almost the full solid angle such that emission into radiative modes can be neglected, i.e., $\gamma_l \approx 0$.

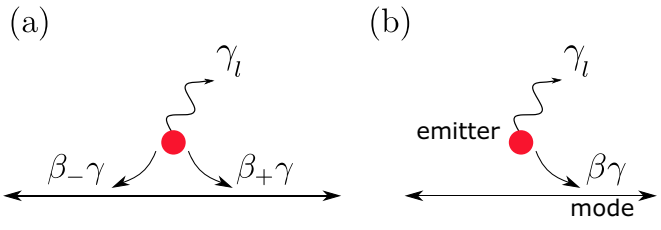

FIG. 1. A single emitter interacting with an optical mode. (a) In principle, an excited emitter can decay through three decay channels: forward or backward into the mode with rates $\beta_+\gamma$ or $\beta_-\gamma$ respectively, or into free space with the rate $\gamma_l = (1-\beta)\gamma$, where $\beta \equiv \beta_+ + \beta_-$, and, in general, $\beta_+ \neq \beta_-$. (b) For the scenario of chiral coupling assumed in Sec. VII, $\beta_- = 0$ and $\beta_+ = \beta$ [20].

V. COLLECTIVE COUPLING IN THE DICKE AND TIMED-DICKE MODEL

Concerning the nature of the collective interaction of many emitters, e.g., an ensemble of identical atoms, with the cavity mode, we have to distinguish two basic cases: either the distance between any two emitters is much smaller than $\lambda/2\pi$, or the interemitter distance is much larger than $\lambda/2\pi$. The two cases are typically described in the framework of Dicke states [21] and timed-Dicke states [22], respectively. Here, λ refers to the wavelength of the light that probes the coupled system.

For the situation where all emitters are separated by less than $\lambda/2\pi$, the cavity field will excite the emitters into the superradiant Dicke state and, assuming the low excitation limit, one excitation is shared between all emitters. Due to

the small separations, the emissions of the individual emitters add up constructively for all emission directions. Thus, the ensemble can be described as an effective "superatom" with a collectively enhanced dipole moment or, equivalently, a collectively enhanced decay rate γ_N. When the near field interaction between the emitters is neglected, the latter is given by $\gamma_N = N\gamma$. According to Eqs. (11) and (12), this results in a collectively enhanced coupling strength to the resonator of $g_N = \sqrt{\gamma_N/\gamma}\ \bar{g}_1$. For this situation, the Tavis-Cummings model typically applies: As g_N^2 and $\gamma_{l,N} = (1-\beta)\gamma_N$ are both proportional to γ_N, their ratio is independent of N. Thus, if Eq. (9) is fulfilled for a single emitter, it is also fulfilled by the ensemble. However, experimentally, is hard to confine emitters to such a small volume. And even if this is achieved, the collective interaction of the emitters with the cavity will not increase the cooperativity: Given that $g_N^2 \propto N$ and $\gamma_N \propto N$, see above, the collective cooperativity of the coupled system, $C_N = g_N^2/(2\,\gamma_{l,N}\,\kappa_0)$, is independent of N.

The situation is different for the case of large emitter-emitter distances. In the low-excitation regime, the collective emitter-light interaction again gives rise to a state with one shared excitation of the ensemble, which is superradiant with respect to the cavity mode and exhibits a collectively enhanced coupling strength, $g_N = \sqrt{N}\bar{g}_1$. However, in contrast to the situation above, the amplitudes for emission into free space now add up incoherently and the emission rate remains unchanged, $\gamma_{l,N} = \gamma_l$. Consequently, for large emitter-emitter distances, the ensemble-resonator cooperativity will increase linearly with N. This is the situation that is aimed for and realized in typical experiments. However, in this case, Eq. (9) will depend on the number of emitters, and the equation will be violated from a certain emitter number onward. Using $g_N = \sqrt{N}\bar{g}_1$ and Eq. (12), we can reformulate Eqs. (8) and (9) and obtain for a ring resonator with chiral coupling

$$\beta N \ll \frac{1}{2}\frac{\nu_{\mathrm{FSR}}}{\gamma}, \tag{13}$$

$$\beta N \ll \tfrac{1}{2}(1-\beta), \tag{14}$$

where $\beta = \sum \beta_n/N$ is the arithmetic mean of β_n of the individual emitters. For most experiments, $\nu_{\mathrm{FSR}} \gg \gamma$ and $\beta \ll 1$. Under these assumptions, condition (14) is always violated first when N increases and takes the simple form

$$\beta N \ll 1/2. \tag{15}$$

For the case of a Fabry-Pérot resonator, we obtain the same expressions as in Eqs. (13)–(15) but with an additional factor $1/2$ on the right-hand side. When considering the interaction of a spatially extended ensemble in a typical cavity QED setup, the assumptions which underlie the TC model therefore no longer hold if βN becomes large. In this case, the modification of the resonator field in a single round trip becomes significant because the single-pass optical depth of the ensemble, given by $OD \approx 4\beta_+ N$ (for $\beta \ll 1$), is no longer small compared to 1. In this case, the local strength of the cavity field depends on its interaction with the preceding emitters, and emitters further along the direction of propagation experience a weaker field.

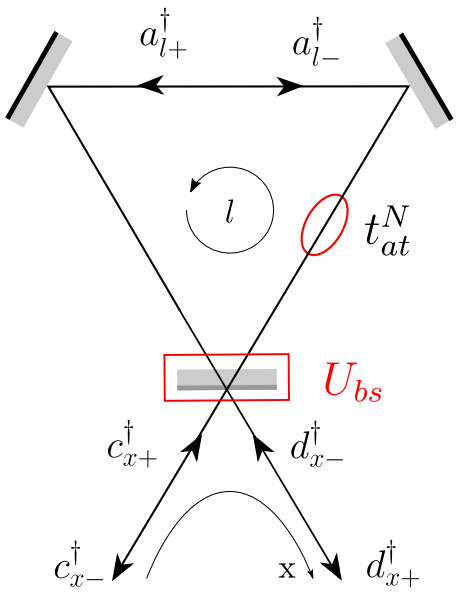

FIG. 2. Sketch of the system under consideration featuring the notations introduced in the main text.

VI. HAMILTONIAN INCLUDING CASCADED EMITTER-LIGHT INTERACTION

In order to derive a Hamiltonian that accounts for the position-dependent resonator field, we follow the formalism in Ref. [23] and treat the resonator mode as a propagating wave that consecutively interacts with two-level quantum emitters. More specifically, we consider the mode of a ring resonator of length L that is coupled to an ensemble of N emitters and include probing and loss; see Fig. 2. The Hamiltonian of this system is given by

$$\begin{aligned}\hat{H}/\hbar = \hat{U}_c &+ \int_{-\infty}^{0} dx[\hat{c}^\dagger_{x_+}(\omega - iv_g\partial_x)\hat{c}_{x_+} + \hat{c}^\dagger_{x_-}(\omega + iv_g\partial_x)\hat{c}_{x_-}] \\ &+ \int_{0}^{+\infty} dx[\hat{d}^\dagger_{x_+}(\omega - iv_g\partial_x)\hat{d}_{x_+} + \hat{d}^\dagger_{x_-}(\omega + iv_g\partial_x)\hat{d}_{x_-}] \\ &+ \int_0^L dl \Bigg\{ [\hat{a}^\dagger_{l_+}(\omega + iv_c\partial_l)\hat{a}_{l_+} + \hat{a}^\dagger_{l_-}(\omega - iv_c\partial_l)\hat{a}_{l_-}] \\ &+ \sum_{n=1}^{N} \delta(l-l_n)[\hat{\sigma}_n^+\hat{\sigma}_n^-(\omega_{\mathrm{a}} - i\gamma_l) \\ &+ V_{n,+}(\hat{a}^\dagger_{l_+}\hat{\sigma}_n^- + \hat{a}_{l_+}\hat{\sigma}_n^+) + V_{n,-}(\hat{a}^\dagger_{l_-}\hat{\sigma}_n^- + \hat{a}_{l_-}\hat{\sigma}_n^+)] \Bigg\}. \end{aligned} \tag{16}$$

Here, the intraresonator field at position l is described by the photon creation and annihilation operators, $\hat{a}^\dagger_{l_+}$ and $\hat{a}_{l_+}$ ($\hat{a}^\dagger_{l_-}$ and $\hat{a}_{l_-}$), for the counterclockwise (clockwise) propagating mode, respectively, with $l \in [0, L[$. $\hat{\sigma}_n^+$ ($\hat{\sigma}_n^-$) is the raising (lowering) operator for emitter n at position l_n, v_g (v_c) is the group velocity of light outside (inside) the resonator, ω_{a} is the emitter's resonance frequency, and $\partial_x = \partial/\partial x$. The coupling strength of the nth emitter to the clockwise and counterclockwise propagating resonator mode is given by $V_{n_\pm} =$

$\sqrt{2v_c\beta_{n\pm}\gamma}$. Here, we assumed that the dispersion relation of the probe field with frequency ω_k and wave number k is approximately linear in the frequency range of interest around the center frequency, i.e., $\omega_{k,\pm} = \omega \pm v_{g,c}k$. The resonator is probed via the incoming and outgoing free-space fields that are denoted by the creation (annihilation) operators $\hat{c}^\dagger_{x_+}$, $\hat{d}^\dagger_{x_-}$ and $\hat{d}^\dagger_{x_+}$, $\hat{c}^\dagger_{x_-}$ ($\hat{c}_{x_+}$, $\hat{d}_{x_-}$ and $\hat{d}_{x_+}$, $\hat{c}_{x_-}$), respectively. These modes are coupled to the resonator modes at the in-coupling mirror, whose effect is given by the beam-splitter matrix

$$\hat{U}_c = \sum_{k=\pm}[t_{\mathrm{rt}}(iv_c r\hat{a}_{L_k}\hat{a}^\dagger_{0_k} + \sqrt{v_g v_c}t\hat{a}_{L_k}\hat{d}^\dagger_{0_k}) + iv_g r\hat{c}_{0_k}\hat{d}^\dagger_{0_k} + \sqrt{v_c v_g}t(\hat{c}_{0_k}\hat{a}^\dagger_{0_k})], \tag{17}$$

where r and t are the amplitude reflection and transmission coefficients of the mirror, which fulfill $r^2 + t^2 = 1$. Note that, just like for the driven JC and TC Hamiltonians [see Eqs. (3) and (6)], the Hamiltonian in Eq. (16) above is non-Hermitian because of the term $-i\gamma_l$, which accounts for photon loss by emitter-induced scattering out of the resonator and because of the factor $t_{\mathrm{rt}} \leqslant 1$ in the definition of U_c, which accounts for resonator round-trip losses. Furthermore, as discussed above, our approach assumes no collectively enhanced emission into free space. With these definitions, the coefficients t_{rt} and r are related to the intrinsic resonator loss rate, κ_0, and the in-coupling rate, κ_{ext}, via $t_{\mathrm{rt}} = \sqrt{1 - 2\kappa_0/\nu_{\mathrm{FSR}}}$ and $r = \sqrt{1 - 2\kappa_{\mathrm{ext}}/\nu_{\mathrm{FSR}}}$.

This description models the successive interaction of the propagating field with N emitters and, thus, naturally considers the modification of the field upon interaction with each individual emitter. Moreover, the model also comprises the possible interaction with several longitudinal cavity modes, which occurs in the superstrong coupling regime. In the next section, we will derive an analytical solution for the steady state in the low excitation limit and discuss how the predictions of this cascaded model differ from that of the TC model and its generalization to more than one mode.

VII. SOLUTIONS IN THE LOW EXCITATION LIMIT

In the following, we want to discuss the differences between the cascaded model and the TC description. Thus, from now on, we assume perfect chiral emitter-resonator coupling [20] which allows us to obtain a simple analytical steady-state solution for the Hamiltonian in Eq. (16). This means we assume that all emitters interact solely with the forward propagating (+ direction) mode via $V_{n,+}$ and set $V_{n-} = 0$ in Eq. (16). Consequently, we get $\beta_{+,n} = \beta_n$ and $\beta_{-,n} = 0$. Details of the derivation can be found in Appendix B. When probing the resonator along the positive x direction, the power reflection at the input mirror ($c^\dagger \to d^\dagger$) reads

$$R = \left|\frac{e^{-i\Delta_c/\nu_{\mathrm{FSR}}}t_{\mathrm{rt}}t_N - r}{e^{-i\Delta_c/\nu_{\mathrm{FSR}}}t_{\mathrm{rt}}t_N r - 1}\right|^2, \tag{18}$$

where

$$t_N = \prod_{n=1}^{N} t_n \tag{19}$$

and t_n is the transmission past emitter n, which is given by (see Appendix B)

$$t_n = 1 - \frac{2\gamma\beta_n}{\gamma + i\Delta_a}. \tag{20}$$

Here, $\Delta_a = \omega_a - \omega$ and $\Delta_c = \omega_c - \omega$ are the probe-emitter and probe-resonator detunings, respectively, and ω_c is the resonator resonance frequency closest to ω_a. For small β_n or small variations between the individual β_n, we can approximate t_N in Eq. (19) by (see Appendix B)

$$t_N = \left(1 - \frac{2\gamma\beta}{\gamma + i\Delta_a}\right)^N, \tag{21}$$

with the mean emitter-mode coupling $\beta = \sum \beta_n/N$. Introducing the complex-valued function

$$\phi(\Delta_a, \Delta_c) = -\frac{\Delta_c}{\nu_{\mathrm{FSR}}} + \arg(t_N) - i\ln|t_N t_{\mathrm{rt}} r| \tag{22}$$

$$\underbrace{\approx}_{\beta\ll 1} -\frac{\Delta_c}{\nu_{\mathrm{FSR}}} + \frac{2\beta N\gamma}{\Delta_a - i\gamma} - i\ln|t_{\mathrm{rt}} r|, \tag{23}$$

we can simplify Eq. (18) and obtain

$$R = \left|\frac{e^{i\phi(\Delta_a,\Delta_c)}/r - r}{e^{i\phi(\Delta_a,\Delta_c)} - 1}\right|^2. \tag{24}$$

With this definition, $\mathrm{Re}\{\phi(\Delta_a, \Delta_c)\}$ corresponds to the phase shift the light acquires in a single round trip in the resonator and $\mathrm{Im}\{\phi(\Delta_a, \Delta_c)\}$ denotes the total round-trip loss.

We note that, even if the system does not exhibit chiral emitter-light coupling, Eqs. (18)–(21) still apply provided that the resonator is probed from one direction, that $\beta \ll 1$, and that a large number of emitters is coupled to the resonator mode at random positions. Under these conditions, collective enhancement only occurs for the direction in which the resonator is probed, and the residual light scattered by the emitters into the counterpropagating resonator mode [24] can be treated as a small loss and does not affect the forward transmission significantly.

Equation (18) or (24) holds for any combination of cavity parameters. For illustration, we consider two limiting cases. First, when conditions (8) and (9) are both fulfilled, the emitters effectively only interact with the single resonator mode closest to the emitter's resonance and the effect of other resonator modes can be neglected. For small detunings ($\Delta_c \ll \nu_{\mathrm{FSR}}$), Eq. (18) can then be simplified (see Appendix D), yielding

$$R = \left|\frac{g_N^2 + (\gamma_l + i\Delta_a)(\kappa_0 - \kappa_{\mathrm{ext}} + i\Delta_c)}{g_N^2 + (\gamma_l + i\Delta_a)(\kappa_0 + \kappa_{\mathrm{ext}} + i\Delta_c)}\right|^2, \tag{25}$$

where $g_N = \sqrt{2N\beta\gamma\nu_{\mathrm{FSR}}}$ is the ensemble-resonator coupling strength. Equation (25) is identical to the predictions of the driven JC and TC model [25]; see Appendix A. Second, for $r \to 0$, i.e., in the waveguide limit where light only takes a single round trip in the resonator, Eq. (18) simplifies to $t_{\mathrm{rt}}^2|t_N|^2$. This expression corresponds to a saturated Lorentzian and is the well-known expression for the transmission spectrum of an optically dense ensemble [26,27].

We note that our approach can also be used to derive the solution for the case where the light-emitter interaction is

described in the Dicke picture. In this case, the power reflection is still described by Eqs. (18) and (24), but the ensemble transmission t_N has to be replaced by its counterpart for the Dicke case

$$t_{N,D} = 1 - \frac{2\gamma_N \beta}{\gamma_N + i\Delta_a} \tag{26}$$

to account for the collectively enhanced decay rate γ_N.

VIII. BEYOND TAVIS-CUMMINGS PHYSICS

In the following, we study the predictions of the TC model and its generalization to more than one mode when its validity conditions (13) and (14) are not fulfilled and compare them with the predictions of our Hamiltonian (16), which generally applies.

A. Excitation spectrum of the coupled system

In the cascaded model, the solution for the intracavity field is given by Eqs. (B5) in Appendix B. In general, the solution depends on the number of emitters the light field has passed within the resonator mode. In the following, we focus on the two main parts: the steady-state resonator field before (ϕ_0) and after (ϕ_N) passing the ensemble. The ratio of the two fields is given by the factor t_N in Eq. (19). For $\beta N \gg 1$ and on resonance ($\Delta_a = \Delta_c = 0$), we obtain for the normalized resonator fields

$$\frac{\phi_0}{\phi_i} = it, \tag{27}$$

$$\frac{\phi_N}{\phi_i} = it\ e^{-2\beta N}, \tag{28}$$

$$\frac{\phi_{TC}}{\phi_i} = it\ \frac{\beta - 1}{2\beta N}, \tag{29}$$

where ϕ_{TC} is the circulating field in the resonator predicted by the Tavis-Cummings model; see Eq. (A7) and ϕ_i is the input field. For large values of βN, these fields differ by many orders of magnitude, which can be seen, e.g., in Fig. 3(a) that shows the normalized intracavity linear photon density predicted by our and the TC models for $\beta N = 10$ as a function of the probe light detuning $\Delta = \Delta_a = \Delta_c$. For larger detunings, the difference between the fields in Eqs. (A7) and (B5) decreases and for $|\Delta| \gg \gamma$, i.e., when the absorption of the ensemble is no longer significant, all fields are approximately identical and the predictions of the two models agree everywhere in the resonator. Figure 3(b) shows in addition the prediction of the power reflection R from the in-coupling mirror calculated from both models for the same parameters as in Fig. 3(a). For large detunings, the predictions of both models agree. In contrast, close to the emitter's resonance, one obtains predictions that quantitatively and qualitatively differ. At resonance and for $\beta N \gg 1$, our cascaded model predicts a reflection $R = r^2$, while the TC model predicts $R = 1$. Furthermore, in our prediction, one observes an additional signature of a resonance that is not present for the TC model. In the following, we study these new resonances in more detail.

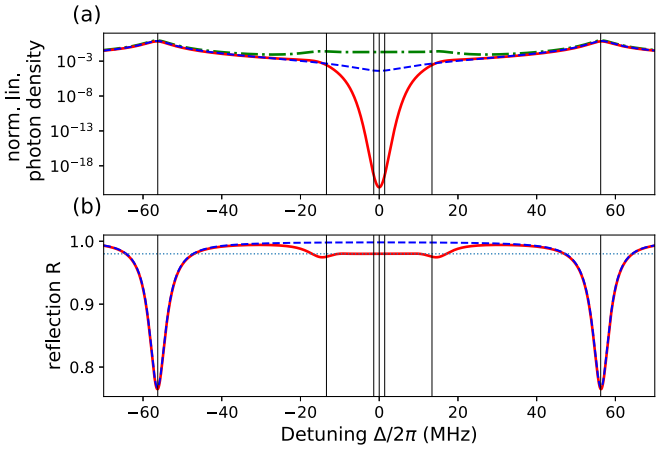

FIG. 3. (a) Normalized linear photon density in the resonator as a function of the light-resonator detuning $\Delta = \Delta_a = \Delta_c$ predicted by the cascaded model for the light before ($|\phi_0|^2$, dash-dotted green curve) and after the emitters ($|\phi_N|^2$, solid red curve) as well as by the TC model (dashed blue curve). The parameters used for the models are $\beta N = 10$, $\nu_{\mathrm{FSR}} = 200$ MHz, $\gamma = 2\pi \times 5$ MHz, and in-coupling mirror power reflectivity $|r|^2 = |t_{rt}|^2 = 98\%$. (b) Corresponding power reflection of the resonator predicted by our (solid red line) and the TC model (dashed blue line). Close to resonance, the predictions for the circulating power differ by many orders of magnitude from each other. In reflection, for large βN, the cascaded model predicts a plateau in the reflection at about $|r|^2$, in contrast to the TC model. For large detuning $\Delta \gg \gamma$, the predictions of the two models for the reflection and the different resonator fields agree with each other. The vertical lines indicate the position of the new resonances predicted by the cascaded model; see Eq. (30) and Fig. 4.

B. Resonances of the coupled system

In general, resonances of the coupled {emitter + cavity} system occur, when the round trip phase is an integer multiple of 2π. For the cascaded model, this is the case for

$$Re\{\phi(\Delta_a, \Delta_c)\} = 2\pi \times q\ , \tag{30}$$

with the integer number q. We first consider the case $g_N \ll \nu_{\mathrm{FSR}}$, i.e., the situation where the interaction of the emitter with the higher order cavity resonances can be neglected. Figures 4(a) and 4(c) show the predicted cavity resonance as a function of βN according to the predictions of the TC model and the cascaded model, respectively. For small βN in Figs. 4(a) and 4(c), we observe the familiar behavior where the central resonance of the cavity splits into two new resonances that, for $g_N \gg (\kappa, \gamma_l)$, are separated by $2g_N$ and for which the splitting increases with $g_N \propto \sqrt{\beta N}$. At the same time, the adjacent longitudinal resonator modes (not shown) are mostly unaffected. However, surprisingly, for large numbers of emitters for which condition (9) or (14) is not fulfilled, the predictions of the two models qualitatively differ. While both models still predict that the splitting of the central line increases $\propto \sqrt{\beta N}$, the cascaded model predicts the occurrence of additional resonances in the spectrum close to the emitter's resonance. As βN increases, more of these new resonances appear.

A physical explanation of the origin of these additional resonances can be obtained when looking at the round-trip

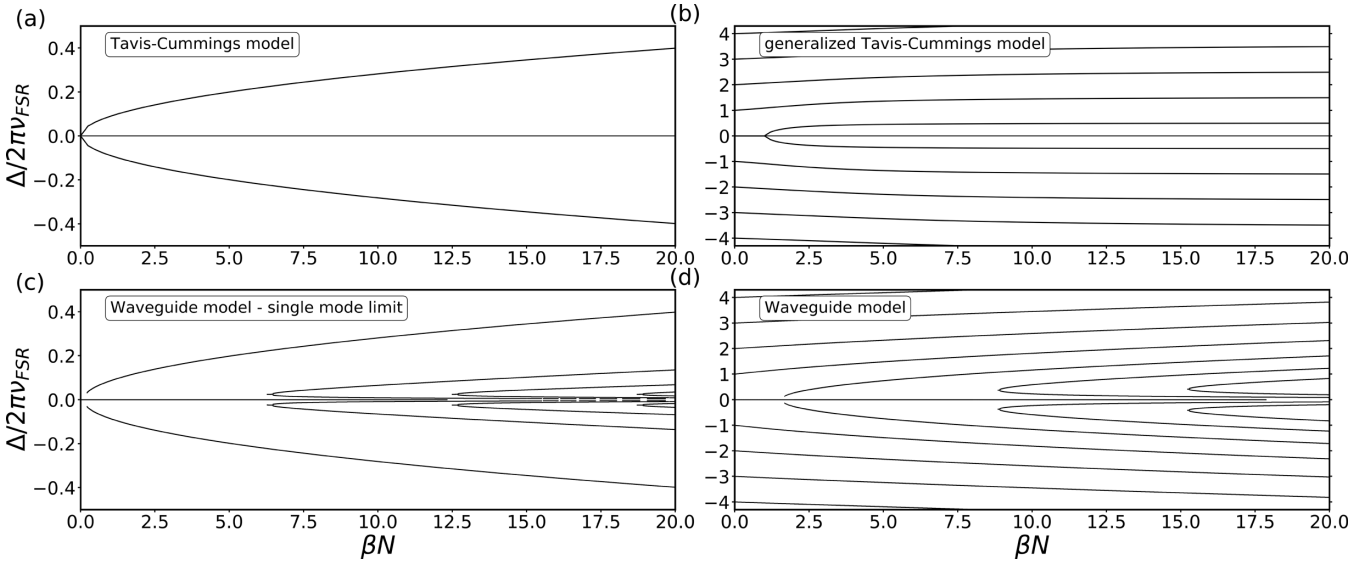

FIG. 4. Positions $\Delta = \Delta_a = \Delta_c$ of the resonances calculated for the Tavis-Cummings model for (a) $g_N \ll \nu_{\mathrm{FSR}}$ ($\nu_{\mathrm{FSR}} = 200$ MHz, $\gamma = 2\pi \times 5$ MHz) and (b) $g_N \gtrsim \nu_{\mathrm{FSR}}$ ($\nu_{\mathrm{FSR}} = 10$ MHz, $\gamma = 2\pi \times 5$ MHz) as a function of βN. Panels (c) and (d) show the predictions of the cascaded model for the same cases and values as in panels (a) and (b), respectively. In panel (a), we see the usual strong coupling prediction, where the central resonance is split by $2g_N \propto \sqrt{N}$. In panel (b), the system enters the superstrong coupling regime, where the splitting saturates at ν_{FSR} and the superstrong coupling spectrum is similar to the empty cavity spectrum but shifted by $\nu_{\mathrm{FSR}}/2$. In contrast to the predictions of the Tavis-Cummings model, the cascaded model [(c) and (d)] predicts the appearance of new resonances for large βN in the region around $\Delta = 0$. This is due to the fact that light undergoes multiple 2π phase shifts in a single resonator roundtrip. Additionally, in panel (d), where both conditions (8) and (9) are violated, contrary to the predictions of Tavis-Cummings, the splitting and shifting of the resonances do not saturate but increase continuously with increasing βN.

phase shift of the light $\mathrm{Re}\{\phi(\Delta_a, \Delta_c)\}$. According to Eq. (23), this phase shift is composed of a propagation and an emitter-induced phase shift. For a single emitter as well as the superatom assumed in the TC model, the phase shift imparted by the emitters to the light is always limited to the range $[-\pi, \pi]$, independently of N. However, when coupling a spatially extended ensemble to the resonator, t_N is given by Eq. (19) and the emitter-induced single-pass phase shift $\arg(t_N)$ can in principle span an unlimited range and, consequently, more solutions to Eq. (30) are found; see Fig. 5.

In the limit where g_N exceeds the free spectral range of the resonator, the emitters strongly interact with different resonator modes and, consequently, the TC model has to be replaced by its generalization to more than one mode, as given in Eq. (10). Figure 4(b) shows the cavity resonances predicted by this model as a function of βN whereas Fig. 4(d) shows the prediction of the cascaded model for the same parameters. In the case shown in Fig. 4(b), one observes that the central resonance starts to split once g_N gets comparable to the loss rate γ_l and the system enters the strong coupling regime. With increasing βN also the adjacent longitudinal resonances are increasingly shifted outward. For very large g_N, the splitting of the central resonance saturates at ν_{FSR} and the shift of all adjacent resonances saturates at $\nu_{\mathrm{FSR}}/2$ with respect to the resonance of the empty resonator. This saturation for large g_N is a consequence of the interaction of the emitter with many modes and can, e.g., be derived from the eigenenergies of the Hamiltonian; see Appendix E.

In contrast to this, the cascaded model does not predict any saturation effect and for $g_N \gg \gamma$ the splitting of the central resonance is simply given by $2g_N = 2\bar{g}_1\sqrt{N}$, i.e., it

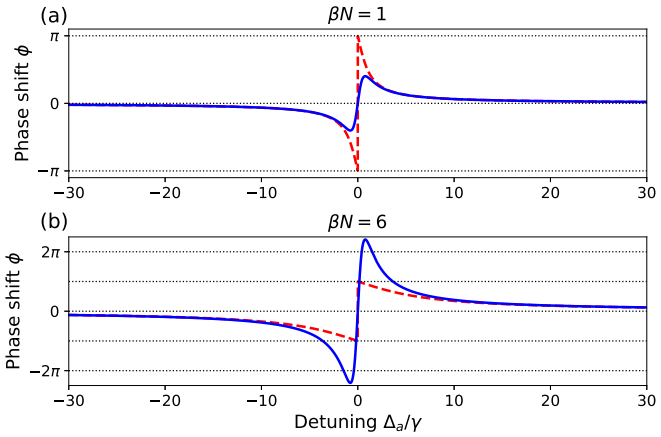

FIG. 5. Single-pass phase shift of the light induced by a two-level quantum emitter as a function of emitter-light detuning Δ_a. (a) The dashed red line shows the results for a perfectly coupled single emitter, i.e., $\beta = 1$ and $N = 1$, as calculated from Eq. (26). The solid blue line represents the predictions of the cascaded model from Eq. (21) with $\beta = 0.2$ and $N = 5$. (b) Same situation as in panel (a) but now for $\beta N = 6$. The dashed red line is the prediction for the Dicke superatom for which the TC model applies. It is calculated from Eq. (26) for $\beta = 1, N = 6$. Interestingly, despite the larger number of emitters, the maximum phase shift of the light imparted by the emitters is not increased compared to panel (a) and remains within $[-\pi, \pi]$. The solid blue line ($\beta = 0.2, N = 30$) shows the predictions of the cascaded model with a maximum phase shift well in excess of $[-\pi, \pi]$.

follows the $\sqrt{N}$ behavior even when the collective coupling exceeds the free spectral range. The other resonator modes are all subject to a shift proportional to $\sqrt{N}$, for $g \gg \nu_{\mathrm{FSR}}$, and show no saturation effect either. Furthermore, similar as in the single-mode situation, the cascaded model predicts the occurrence of new resonances close to the emitter's resonance.

In summary, when comparing the resonance frequencies predicted by the TC model and our cascaded model, qualitative differences occur already in the weak driving limit considered here. These differences are present for the single-mode as well as the multimode situation, where in both cases, the cascaded model predicts the occurrence of new resonances that are not present in the TC model. Furthermore, for the multimode situation, the TC model predicts a saturation of the shift of the cavity resonances which does not occur in our description. We note that the new resonances emerge close to or within the absorption profile of the ensemble where the propagating cavity field is subject to strong absorption. As a consequence, they are expected to only give rise to a low-contrast modulation of the power reflection signal. This holds in particular for the branches that shift toward the emitter's resonance.

IX. EXPERIMENTAL VERIFICATION

To experimentally illustrate the breakdown of the Tavis-Cummings model, we experimentally investigate the situation where the conditions (8) and (9) break down using an experimental platform in the superstrong coupling regime, which we reported on in Ref. [6]. Compared to the measurements presented in this previous publication, we could substantially increase the collective coupling strength, which allows us to now highlight the deviation from the TC model. The experiment consists of a cloud of laser-cooled Cs atoms coupled to a 30-m-long ring fiber resonator ($\nu_{\mathrm{FSR}} = 7.1$ MHz) via a nanofiber-based optical interface. The effective number of atoms that are coupled to the resonator mode reaches up to $\approx$2300, thereby giving rise to a maximum $\beta N = 12.96$ (or $g_N = 2\pi \times 8.74$ MHz). We measure the loaded cavity spectra for a range of different collective coupling strengths, scanning the frequency of the probe field over many free spectral ranges and measuring its power reflection with a single photon counter. The result of this measurement is summarized in Fig. 6.

Figures 6(a) and 6(b) show the measured spectrum together with the predictions of the TC model and the cascaded model, respectively. Whereas the positions of the cavity resonances do not follow the predictions of the Tavis-Cummings approach, theory and experiment agree well for the cascaded model. Specifically, we observe that the shifts of the resonances do not saturate as the collective coupling strength increases and its dependence on βN agrees well with the prediction from the cascaded model (solid black lines). Furthermore, the maximum shift observed, e.g., for the +1st order, exceeds $\nu_{\mathrm{FSR}}/2$ and the fit splitting reveals $2g_N \approx 2.3\nu_{\mathrm{FSR}}$. These observations exceed the predictions of the TC approach significantly. We note that, due to the low finesse of the resonator, the predicted contrast of the additional resonances for our experimental settings is only about 0.1%,

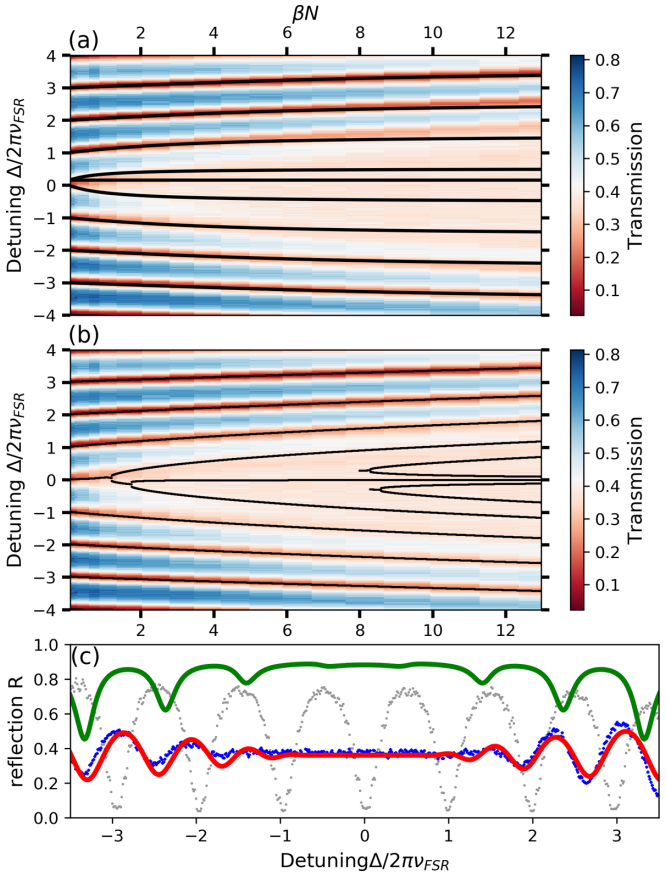

FIG. 6. Experimentally measured reflection spectra of a ring resonator coupled to an optically dense cloud of atoms. The black solid lines indicate the resonance frequencies predicted by the generalized TC model in panel (a) and the cascaded model in panel (b), both for $\gamma/2\pi = 2.61$ MHz, $\beta = 0.005$, and $\nu_{\mathrm{FSR}} = 7.1$ MHz. (c) Cut through the data (dark blue dots) presented in panels (a) and (b) for $\beta N = 12.4$, with a theory curve using the generalized TC model (green, solid upper line) and a fit to the cascaded model (red, solid lower line), using Eq. (18). Note that for all theory plots a cavity-atom detuning $\Delta_{ca} = 1.12$ MHz is considered, that was present during the measurement. It becomes apparent that the cascaded model agrees well with the experimental data and, for the large coupling strength depicted here, we observe the splitting of the central resonance exceeding the limit of ν_{FSR} and the shift does not saturate, unlike in the TC prediction. Note that the predicted additional resonances in panel (b) cannot be discerned in the experimental data due to their small contrast and the limited signal to noise of our measurement. The shifting of the first higher resonance exceeds $\nu_{\mathrm{FSR}}/2$ as can be seen by comparison to the spectrum of the empty resonator (light gray dots), indicating operation in the superstrong coupling regime.

which is below our experimental signal to noise ratio. Thus, the new resonances cannot be discerned in our data.

X. SUMMARY AND CONCLUSION

In this article, we derived quantitative conditions under which the Tavis-Cummings model fails to correctly describe the interaction of an ensemble of two-level quantum emitters with a single optical mode. Our analysis shows that the valid-

ity of the Tavis-Cummings model breaks down as soon as the single-pass optical depth of the ensemble approaches OD ≈ 1. In this case, the collective interaction of the emitters with the resonator mode needs to be accounted for by considering the successive interaction of the propagating cavity field with each emitter in the ensemble, because the field is significantly altered by each of these interaction events. We then presented a more general theoretical model that can be applied for describing cQED in all parameter ranges. Using this cascaded model, we analytically derived the steady-state solution in the low power limit and compared it to the predictions of the Tavis-Cummings model. We found qualitative differences between the predictions of the two models concerning the intracavity linear photon density and the reflection spectrum of the coupled emitter-cavity system. Around the emitter's resonance the cascaded model predicts a position-dependent photon density that for $\beta N \gg 1$ can deviate by several orders of magnitude from the photon density derived from the TC model. Furthermore, the Tavis-Cumming model predicts that, irrespective of the number of coupled emitters, the splitting of the central resonance cannot exceed the resonator's free spectral range. In contrast, the cascaded model predicts that the splitting is not limited and continues to grow as the number of emitters increases. Moreover, with increasing number of emitters, the cascaded model predicts a growing number of additional resonances, which are missing by the Tavis-Cummings model. These resonances occur because, for large ensembles, the single-pass phase shift of the cavity field induced by the quantum emitters is in principle not limited. This feature cannot be captured by the Tavis-Cummings model, where the largest possible phase shift is $\pm\pi$. We compare our findings to experimentally measured reflection spectra of a 30-m-long optical ring resonator, which is coupled with a high optical depth atomic ensemble. The measured spectra agree well with the predictions of the cascaded model and qualitatively disagree with the Tavis-Cummings model.

Our approach is not limited to a concrete realization of the cavity, the quantum emitter, or the emitter-light coupling mechanism. Consequently, our findings are relevant for all theoretical and experimental studies, in which the number of resonator-coupled emitters reaches or exceeds $1/(2\beta)$; see Eq. (15). In this case, the Tavis-Cummings model should be taken with precaution. This particularly applies to experiments that study superradiance [28–31] or that make use of cooperative effects to enhance the performance of quantum memories and, thus, invariantly aim for high single-pass optical depths. Adding a cavity with the aim of enhancing the performance then inevitably sets these experiments into a regime where the Tavis-Cummings model cannot be applied. Instead, in general, our approach is required for correctly modeling the system's properties. Furthermore, in the superstrong coupling regime, non-Markovian dynamics has been predicted where, e.g., pulsed revivals rather than conventional Rabi oscillations are expected [32]. However, this non-Markovian behavior requires high single-pass optical depths. Thus, the Tavis-Cummings model cannot be expected to hold in this regime while our description is well suited in view of its wide range of applicability. We note that Eq. (15) can already be violated for a single two-level emitter for $\beta \gtrsim 1/2$. This shows that even the single-emitter cavity system can only be described correctly by the JC model for the case of small β, i.e., for large scattering losses into the environment. Consequently, the case of an emitter perfectly coupled to a cavity mode ($\beta = 1$) is not covered by the JC model, which will be discussed in Ref. [33], where we study in detail the situation of a single emitter coupled with high β to a Fabry-Pérot or ring resonator.

In this paper, we limited our discussion to the linear regime of low excitation where at most one photon is present in the cavity. Under these assumptions, we can derive analytical solutions for the system. Already here, we observe qualitative deviations between the Tavis-Cummings approximation and the cascaded model. However, one of the main reasons for using optical cavities is the enhancement of nonlinear effects. In this context, we also expect to observe qualitative differences concerning the nonlinear properties of the system. For example, it has recently been shown theoretically and experimentally that the transmission of light through an atomic ensemble with a large optical depth leads to the generation of photon correlations and squeezing through the collective nonlinear response of the atoms [34–37]. The physics underlying these effects is already contained in our Hamiltonian. This illustrates that the theoretical framework presented in this article has consequences and applications that go well beyond the presented examples. It therefore has the potential to reveal new physics that cannot be captured by the Jaynes- and Tavis-Cummings models.

ACKNOWLEDGMENTS

We acknowledge financial support by the Alexander von Humboldt Foundation in the framework of an Alexander von Humboldt Professorship endowed by the Federal Ministry of Education and Research and by the Austrian Science Fund (NanoFiRe Grant Project No. P 31115).

APPENDIX A: STRONG COUPLING IN THE JC (TC) MODEL

In order to derive the steady state of a resonator coupled to a single emitter, we use a photon transport approach [23] to quantum mechanically describe the resonator probing fields. The Hamiltonian of this system is given by

$$\hat{H} = \hat{H}_{\mathrm{JC}'} + \hat{U}_{\mathrm{probe}}, \tag{A1}$$

where the first term describes the interaction of a single emitter with the cavity field. It includes loss from photons scattered into noncavity modes by the emitter ($-i\gamma_l$) and loss from the cavity implementation ($-i\kappa_0$) and is given by

$$\hat{H}_{\mathrm{JC}'}/\hbar = (\Delta_a - i\gamma_l)\hat{\sigma}^+\hat{\sigma}^- + (\Delta_c - i\kappa_0)\hat{a}^\dagger\hat{a} + g(\hat{a}^\dagger\hat{\sigma}^- + \hat{a}\hat{\sigma}^+). \tag{A2}$$

Here, $\hat{a}^\dagger$ ($\hat{a}$) is the cavity photon creation (annihilation) operator, $\Delta_c = \omega_c - \omega$ is the cavity-probe detuning, $\Delta_a = (\omega_a - \omega)$ is the emitter-probe detuning, and g is the coupling strength. The probing term describes the coupling of a driving field $\hat{c}_x^\dagger$ to the cavity via

$$\frac{\hat{U}_{\mathrm{probe}}}{\hbar} = \int_{-\infty}^{\infty} dx[\hat{c}_x^\dagger(\omega_0 - iv_g\partial_x)\hat{c}_x + V_{\mathrm{cav}}\delta(x)(\hat{a}^\dagger\hat{c}_x + \hat{a}\hat{c}_x^\dagger)], \tag{A3}$$

where $V_{\rm cav} = \sqrt{2\kappa_{\rm ext} v_g}$ is the coupling strength between cavity and the driving field. In the weak driving regime, we obtain the steady-state solution of $\hat{H}|\Psi\rangle = E|\Psi\rangle$ by using a general single excitation wave function

$$|\Psi\rangle = \left[\int dx \phi_{\rm c}(x)\hat{c}_x^\dagger + \phi_{\rm cav} a^\dagger + \phi_{\rm at}\hat{\sigma}^+\right]|0\rangle. \quad \text{(A4)}$$

The results for the steady-state values for the amplitude of the output (input) field, ϕ_o (ϕ_i), the emitter's excitation amplitude, $\phi_{\rm at}$, and the cavity field amplitude, $\phi_{\rm cav}$, are given by

$$\frac{\phi_o}{\phi_i} = \frac{g^2 + (\gamma_l + i\Delta_a)(\kappa_0 - \kappa_{\rm ext} + i\Delta_c)}{g^2 + (\gamma_l + i\Delta_a)(\kappa_0 + \kappa_{\rm ext} + i\Delta_c)}, \quad \text{(A5)}$$

$$\frac{\phi_{\rm at}}{\phi_i} = \frac{-g\sqrt{2v_g\kappa_{\rm ext}}}{g^2 + (\gamma_l + i\Delta_a)(\kappa_0 + \kappa_{\rm ext} + i\Delta_c)}, \quad \text{(A6)}$$

$$\frac{\phi_{\rm cav}}{\phi_i} = \frac{-i\sqrt{2v_g\kappa_{\rm ext}}(\gamma_l + i\Delta_a)}{g^2 + (\gamma_l + i\Delta_a)(\kappa_0 + \kappa_{\rm ext} + i\Delta_c)}, \quad \text{(A7)}$$

$$\frac{\phi_{\rm at}}{\phi_{\rm cav}} = \frac{-ig}{\gamma_l + i\Delta_a}, \quad \text{(A8)}$$

where $|\frac{\phi_{\rm at}}{\phi_{\rm cav}}|^2 = \frac{g^2}{\gamma_l^2 + \Delta_a^2}$ is the cavity-induced emitter excitation probability, such that the emitter-induced loss from the cavity on resonance can be calculated to be g^2/γ_l, appearing in condition (9). The results above apply for both, the JC and TC Hamiltonian with $g = g_1$ or $g = g_N$.

APPENDIX B: CHIRAL COUPLING TO A RING CAVITY

Here we outline the derivation of Eq. (18) in the main text. For chiral interaction, the Hamiltonian in Eq. (16) can be simplified by neglecting the resonator mode $\hat{a}_{l_-}^\dagger$ ($\hat{a}_{l_-}$) that is not coupled to the emitters ($V_{n-} = 0$) and consequently $\hat{c}_-^\dagger, \hat{c}_- = 0$ and $\hat{d}_-^\dagger, \hat{d}_- = 0$. This gives

$$\begin{aligned}\hat{H}/\hbar = \hat{U}_c &+ \int_{-\infty}^{0} dx[\hat{c}_{x_+}^\dagger(\omega - iv_g\partial_x)\hat{c}_{x_+}] \\ &+ \int_0^{+\infty} dx[\hat{d}_{x_+}^\dagger(\omega - iv_g\partial_x)\hat{d}_{x_+}] \\ &+ \int_0^L dl\Bigg\{[\hat{a}_{l_+}^\dagger(\omega + iv_c\partial_l)\hat{a}_{l_+}] \\ &+ \sum_{n=1}^{N}\delta(l - l_n)[\hat{\sigma}_n^+\hat{\sigma}_n^-(\omega_{\rm a} - i\gamma_l) \\ &+ V_{n+}(\hat{\sigma}_n^+\hat{a}_{l_+} + \hat{\sigma}_n^-\hat{a}_{l_+}^\dagger)]\Bigg\}. \quad \text{(B1)}\end{aligned}$$

The general single excitation wave function of the system is of the form

$$\begin{aligned}|\Psi\rangle = \Bigg[&\int_{-\infty}^{0} dx\phi_c(x)\hat{c}_{x_+}^\dagger + \int_0^\infty dx\phi_d(x)\hat{d}_{x_+}^\dagger \\ &+ \int_0^L dl\phi_a(l)\hat{a}_{l_+}^\dagger + \sum_{n=1}^{N}\phi_{{\rm at},n}\hat{\sigma}_n^+\Bigg]|0\rangle. \quad \text{(B2)}\end{aligned}$$

To obtain the steady-state solution, we make the ansatz that the fields can be described as propagating plane waves with wave number k of the form

$$\begin{aligned}\phi_c(x) &= e^{ikx}\phi_c\Theta(-x), \\ \phi_d(x) &= e^{ikx}\phi_d\Theta(x), \\ \phi_a(l) &= e^{-ikl}\sum_{n=0}^{N}\phi_n\Theta(l - l_n)\Theta(l_{n+1} - l), \quad \text{(B3)}\end{aligned}$$

where $l_0 = 0$ and $l_{N+1} = L$, Θ is the Heaviside step function, and ϕ_c and ϕ_d are complex numbers. Here, the nth emitter couples to the resonator at position l_n with ϕ_n being the cavity field after the nth emitter and $\phi_{{\rm at},n}$ being the excitation amplitude of emitter n. For simplicity, we set $v_g = v_c$. Using these relations, one can unambiguously solve the eigenvalue problem $\hat{H}|\Psi\rangle = E|\Psi\rangle$. Injecting the wave-function ansatz into the Schrödinger equation, we obtain a set of coupled equations

$$\begin{aligned}0 &= -iv_g\frac{\phi_d}{2} - v_g t_{\rm rt} t\frac{\phi_N}{2}e^{-ikL} + iv_g r\frac{\phi_c}{2}, \\ 0 &= iv_g\frac{\phi_0}{2} - iv_g t_{\rm rt} r\frac{\phi_N}{2}e^{-ikL} + v_g t\frac{\phi_c}{2}, \\ 0 &= -iv_g(\phi_n - \phi_{n-1})e^{-ikl_n} + V_{n+}\phi_{{\rm at},n}, \\ 0 &= \frac{V_{n+}}{2}(\phi_n + \phi_{n-1})e^{-ikl_n} + (\Delta_a - i\gamma_l)\phi_{{\rm at},n}. \quad \text{(B4)}\end{aligned}$$

For the waveguide-emitter coupling $V_{n+} = \sqrt{2\beta_n\gamma v_g}$ and the emitter-field detuning $\Delta_a = (\omega_{\rm a} - \omega)$, we can solve the set of equations above. For the resonator fields, we get

$$\begin{aligned}\frac{\phi_n}{\phi_{n-1}} &= 1 - \frac{2\beta_{+,n}\gamma}{\gamma + i\Delta_a} = t_n, \quad n \neq 0, \\ \frac{\phi_0}{\phi_c} &= \frac{-it}{e^{-ikL} r t_N t_{\rm rt} - 1}. \quad \text{(B5)}\end{aligned}$$

For the field at the output of the probed emitter-cavity system, we get

$$\frac{\phi_d}{\phi_c} = \frac{t_N t_{\rm rt} e^{-ikL} - r}{t_N t_{\rm rt} r e^{-ikL} - 1}. \quad \text{(B6)}$$

Using $kL = \Delta_c/\nu_{\rm FSR}$ we obtain for the power reflection of a loaded ring resonator Eq. (18)

$$R = \left|\frac{\phi_d}{\phi_c}\right|^2 = \left|\frac{e^{-i\Delta_c/\nu_{\rm FSR}} t_{\rm rt} t_N - r}{e^{-i\Delta_c/\nu_{\rm FSR}} t_{\rm rt} t_N r - 1}\right|^2. \quad \text{(B7)}$$

Apart from the resonator fields between the emitters in Eq. (B5), all quantities only depend on the total single-pass transmission t_N through the whole ensemble, which is given by

$$t_N = \prod_{n=1}^{N} t_n. \quad \text{(B8)}$$

For β_n sufficiently small or sufficiently small variations of β_n we can approximate t_N via

$$t_N = 1 - \sum_n \tilde{\beta}_n + \sum_{n<m}\tilde{\beta}_n\tilde{\beta}_m - \ldots$$

$$= 1 - \underbrace{\sum_n \tilde{\beta}_n}_{=N\tilde{\beta}} + \underbrace{\Big(\sum_n \tilde{\beta}_n\Big)^2 - \sum_n \tilde{\beta}_n^2}_{\approx \frac{1}{2}(N^2-N)\beta^2} - \ldots$$

$$\approx \sum_n \binom{N}{n}(-\tilde{\beta})^n = (1-\tilde{\beta})^N, \tag{B9}$$

where we used the shorthand notation $\tilde{\beta}_n = 2\beta_n\gamma/(\gamma + i\Delta_a)$ and $\tilde{\beta} = 2\beta\gamma/(\gamma + i\Delta_a)$, with $\beta = \sum\beta_n/N$ describing the mean emitter-mode coupling. We note that for large detuning $\Delta_a > \gamma$, this approximation is always fulfilled.

APPENDIX C: COUPLING STRENGTH g AND β FACTOR

To compare the description of the cascaded model to the Jaynes- and Tavis-Cummings models, we need an expression linking the characteristic coupling parameters g_1 and β with the definition $\langle\hat{a}^\dagger\hat{a}\rangle = \langle\hat{n}\rangle$, where $\hat{n}$ is the number operator quantifying the mean number of photons inside the cavity and $\hat{a}^\dagger$ ($\hat{a}$) is the photon creation (annihilation) operator in the Jaynes-Cummings Hamiltonian. For the cascaded model, the mean intracavity photon number is $\langle\int_0^L dl\,\hat{a}_l^\dagger\hat{a}_l\rangle = \langle\hat{n}\rangle$. With this we can identify $V_{n+}^2/L = g^2$, which leads to

$$g^2 = 4\beta\gamma\nu_{\mathrm{FSR}} \tag{C1}$$

for an emitter placed inside an antinode of the cavity field in a Fabry-Pérot cavity (symmetric coupling) and

$$g^2 = 2\beta\gamma\nu_{\mathrm{FSR}} \tag{C2}$$

for a ring cavity, where we assumed chiral coupling.

APPENDIX D: SOLUTIONS OF OUR CASCADED MODEL FOR LARGE ν_{FSR}

From the reflection in the cascaded real-space formalism in Eq. (18), one can reproduce the reflection spectra calculated from the Jaynes- and Tavis-Cummings model for a resonator coupled strongly to an ensemble of quantum emitters, for $\beta N < 1$. At first, we substitute for $\beta_n\gamma$ using $g^2 = 2\beta_n\gamma\nu_{\mathrm{FSR}}$ as

$$t_n = 1 - \frac{2\beta_n\gamma}{\gamma + i\Delta_a} = 1 - \frac{2g^2}{g^2 + 2\nu_{\mathrm{FSR}}(\gamma_l + i\Delta_a)}. \tag{D1}$$

For single-mode interaction, where $\Delta_c \ll \nu_{\mathrm{FSR}}$, a condition satisfied in most conventional cQED experiments, we can restrict the derivation to first order in ν_{FSR} and obtain for the reflection from the incoupling mirror

$$R = \left|\frac{g^2 + (\gamma_l + i\Delta_a)(\kappa_0 - \kappa_{\mathrm{ext}} + i\Delta_c)}{g^2 + (\gamma_l + i\Delta_a)(\kappa_0 + \kappa_{\mathrm{ext}} + i\Delta_c)}\right|^2, \tag{D2}$$

the same expression as from Jaynes- and Tavis-Cummings as derived in Eq. (A5) for $g = g_1$ or $g = g_N$, respectively.

APPENDIX E: MULTIMODE EXTENSIONS OF THE JAYNES- AND TAVIS-CUMMINGS MODELS

Starting from the standard Jaynes-Cummings approach, Eq. (1), the generalization to many modes is

$$\frac{\hat{H}}{\hbar} = \omega_{\mathrm{at}}\hat{\sigma}^+\hat{\sigma}^- + \sum_j[\omega_j\hat{a}_j^\dagger\hat{a}_j + g_j(\hat{a}_j^\dagger\hat{\sigma}^- + \hat{a}_j\hat{\sigma}^+)], \tag{E1}$$

where $\hat{a}_j^\dagger$ creates a photon in the jth mode of the resonator and g_j is the coupling strength between the emitter and the cavity mode j. In a similar way, we can apply the same method to the Tavis-Cummings model

$$\frac{\hat{H}}{\hbar} = \omega_{\mathrm{at}}\hat{S}^+\hat{S}^- + \sum_j[\omega_j\hat{a}_j^\dagger\hat{a}_j + g_{N,j}(\hat{a}_j^\dagger\hat{S}^- + \hat{a}_j\hat{S}^+)], \tag{E2}$$

where we substituted the operators $\hat{S}^\pm = 1/\sqrt{N}\sum_n\hat{\sigma}_n^\pm$, to take a collective emitter-resonator interaction into account. In order to calculate the eigenvalue spectrum of the Hamiltonian, we now consider an equally distributed mode spacing of the resonator around the emitter's resonance as $\omega_j = j\omega_{\mathrm{FSR}} + \Delta_a$, where we define ω_0 as the resonance closest to the emitter's resonance. The resonator modes are separated by the free spectral range $\omega_{\mathrm{FSR}} = 2\pi\nu_{\mathrm{FSR}}$ and $\Delta_a = \omega_{\mathrm{at}} - \omega_0$ is the emitter-resonator detuning. Furthermore, for simplicity, we assume that the emitters couple with equal strength to all cavity modes with $g = g_{N,j}$ which is, e.g., the case for a ring resonator. In order to solve the Schrödinger equation $\hat{H}|\Psi\rangle = \hbar\omega|\Psi\rangle$, we make a single-excitation wave-function ansatz $|\Psi\rangle = \sum_j\alpha_j\hat{a}_j^\dagger + \beta\hat{\sigma}^+|0\rangle$. Plugging the ansatz into the time-independent Schrödinger equation and comparing coefficients leads to

$$\alpha_j = \frac{g\beta}{\omega - j\omega_{\mathrm{FSR}} - \Delta_a} \quad \text{and} \tag{E3}$$

$$\beta = \frac{g}{\omega}\sum_{j=1}^{N}\alpha_j. \tag{E4}$$

From this, we can formulate an eigenvalue equation

$$1 = \frac{g^2}{\omega}\sum_{j=-M}^{M}\frac{1}{\omega - j\,\omega_{\mathrm{FSR}} - \Delta_a}, \tag{E5}$$

having $2(M+1)$ solutions, where $2M+1$ is the number of modes considered. In the limiting case of very large coupling strength $g \gg \omega_{\mathrm{FSR}}$, we can make an ansatz for $\omega = m\omega_{\mathrm{FSR}}$ ($m \in \mathbb{R}$) and approximate $\omega_{\mathrm{FSR}}^2/g^2 \to 0$. With this, we arrive at

$$0 = \sum_{j=-M}^{M}\frac{1}{m - (j + \Delta_a/\nu_{\mathrm{FSR}})}. \tag{E6}$$

For $M \to \infty$, this equation can be solved for any mode k ($k \in \mathbb{N}$) by $m_k = \frac{1}{2} + \Delta_a/\omega_{\mathrm{FSR}} + k$. Consequently, for a coupled multimode emitter-resonator system, we find the position of the new resonances of the {emitter + cavity} system at the frequencies

$$\tilde{\omega}_k = \omega_k + \tfrac{1}{2}\omega_{\mathrm{FSR}}, \tag{E7}$$

where k is the resonance's mode number and ω_k the frequency of the bare cavity resonance. All resonances are shifted by $\omega_{\mathrm{FSR}}/2$ from their position of the bare cavity system, where the shift saturates.

[1] R. J. Thompson, G. Rempe, and H. J. Kimble, Observation of Normal-Mode Splitting for an Atom in an Optical Cavity, Phys. Rev. Lett. **68**, 1132 (1992).

[2] M. Brune, F. Schmidt-Kaler, A. Maali, J. Dreyer, E. Hagley, J. M. Raimond, and S. Haroche, Quantum Rabi Oscillation: A Direct Test of Field Quantization in a Cavity, Phys. Rev. Lett. **76**, 1800 (1996).

[3] A. Reiserer and G. Rempe, Cavity-based quantum networks with single atoms and optical photons, Rev. Mod. Phys. **87**, 1379 (2015).

[4] H. Ritsch, P. Domokos, F. Brennecke, and T. Esslinger, Cold atoms in cavity-generated dynamical optical potentials, Rev. Mod. Phys. **85**, 553 (2013).

[5] A. K. Tuchman, R. Long, G. Vrijsen, J. Boudet, J. Lee, and M. A. Kasevich, Normal-mode splitting with large collective cooperativity, Phys. Rev. A **74**, 053821 (2006).

[6] A. Johnson, M. Blaha, A. E. Ulanov, A. Rauschenbeutel, P. Schneeweiss, and J. Volz, Observation of Collective Superstrong Coupling of Cold Atoms to a 30-m-Long Optical Resonator, Phys. Rev. Lett. **123**, 243602 (2019).

[7] L. W. Clark, N. Schine, C. Baum, N. Jia, and J. Simon, Observation of Laughlin states made of light, Nature (London) **582**, 41 (2020).

[8] F. Brennecke, T. Donner, S. Ritter, T. Bourdel, M. Köhl, and T. Esslinger, Cavity QED with a Bose-Einstein condensate, Nature (London) **450**, 268 (2007).

[9] Y. Colombe, T. Steinmetz, G. Dubois, F. Linke, D. Hunger, and J. Reichel, Strong atom–field coupling for Bose-Einstein condensates in an optical cavity on a chip, Nature (London) **450**, 272 (2007).

[10] V. D. Vaidya, Y. Guo, R. M. Kroeze, K. E. Ballantine, A. J. Kollár, J. Keeling, and B. L. Lev, Tunable-range, photon-mediated atomic interactions in multimode cavity QED, Phys. Rev. X **8**, 011002 (2018).

[11] S. C. Schuster, P. Wolf, S. Ostermann, S. Slama, and C. Zimmermann, Supersolid Properties of a Bose-Einstein Condensate in a Ring Resonator, Phys. Rev. Lett. **124**, 143602 (2020).

[12] D. Meiser and P. Meystre, Superstrong coupling regime of cavity quantum electrodynamics, Phys. Rev. A **74**, 065801 (2006).

[13] F. Ripka, H. Kübler, R. Löw, and T. Pfau, A room-temperature single-photon source based on strongly interacting Rydberg atoms, Science **362**, 446 (2018).

[14] X.-X. Hu, C.-L. Zhao, Z.-B. Wang, Y.-L. Zhang, X.-B. Zou, C.-H. Dong, H. X. Tang, G.-C. Guo, and C.-L. Zou, Cavity-enhanced optical controlling based on three-wave mixing in cavity-atom ensemble system, Opt. Express **27**, 6660 (2019).

[15] M. Tavis and F. W. Cummings, Exact solution for an N-molecule-radiation-field Hamiltonian, Phys. Rev. **170**, 379 (1968).

[16] M. Tavis and F. W. Cummings, Approximate solutions for an N-molecule-radiation-field Hamiltonian, Phys. Rev. **188**, 692 (1969).

[17] E. T. Jaynes and F. W. Cummings, Comparison of quantum and semiclassical radiation theories with application to the beam maser, IEEE **51**, 89 (1963).

[18] J. Lee, G. Vrijsen, I. Teper, O. Hosten, and M. A. Kasevich, Many-atom–cavity QED system with homogeneous atom–cavity coupling, Opt. Lett. **39**, 4005 (2014).

[19] Y. Jiang, Y. Mei, Y. Zou, Y. Zuo, and S. Du, Intracavity cold atomic ensemble with high optical depth, Rev. Sci. Instrum. **90**, 13105 (2019).

[20] P. Lodahl, S. Mahmoodian, S. Stobbe, P. Schneeweiss, J. Volz, A. Rauschenbeutel, H. Pichler, and P. Zoller, Chiral quantum optics, Nature (London) **541**, 473 (2017).

[21] R. H. Dicke, Coherence in spontaneous radiation processes, Phys. Rev. **93**, 99 (1954).

[22] M. O. Scully, E. S. Fry, C. H. Raymond Ooi, and K. Wódkiewicz, Directed Spontaneous Emission from an Extended Ensemble of n Atoms: Timing is Everything, Phys. Rev. Lett. **96**, 010501 (2006).

[23] J.-T. Shen and S. Fan, Theory of single-photon transport in a single-mode waveguide. I. Coupling to a cavity containing a two-level atom, Phys. Rev. A **79**, 023837 (2009).

[24] D. Reitz, C. Sayrin, B. Albrecht, I. Mazets, R. Mitsch, P. Schneeweiss, and A. Rauschenbeutel, Backscattering properties of a waveguide-coupled array of atoms in the strongly non-paraxial regime, Phys. Rev. A **89**, 031804(R) (2014).

[25] H. Carmichael, *An Open Systems Approach to Quantum Optics* (Springer Science & Business Media, Berlin, 2009).

[26] G. Sagué, E. Vetsch, W. Alt, D. Meschede, and A. Rauschenbeutel, Cold-Atom Physics Using Ultrathin Optical Fibers: Light-Induced Dipole Forces and Surface Interactions, Phys. Rev. Lett. **99**, 163602 (2007).

[27] E. Vetsch, D. Reitz, G. Sagué, R. Schmidt, S. T. Dawkins, and A. Rauschenbeutel, Optical Interface Created by Laser-Cooled Atoms Trapped in the Evanescent Field Surrounding an Optical Nanofiber, Phys. Rev. Lett. **104**, 203603 (2010).

[28] M. O. Araújo, I. Krešić, R. Kaiser, and W. Guerin, Superradiance in a Large and Dilute Cloud of Cold Atoms in the Linear-Optics Regime, Phys. Rev. Lett. **117**, 073002 (2016).

[29] G. Ferioli, A. Glicenstein, L. Henriet, I. Ferrier-Barbut, and A. Browaeys, Storage and release of subradiant excitations in a dense atomic cloud, Phys. Rev. X **11**, 021031 (2021).

[30] P. Solano, P. Barberis-Blostein, F. K. Fatemi, L. A. Orozco, and S. L. Rolston, Super-radiance reveals infinite-range dipole interactions through a nanofiber, Nat. Commun. **8**, 1857 (2017).

[31] C. C. Kwong, T. Yang, M. S. Pramod, K. Pandey, D. Delande, R. Pierrat, and D. Wilkowski, Cooperative Emission of a Coherent Superflash of Light, Phys. Rev. Lett. **113**, 223601 (2014).

[32] D. O. Krimer, M. Liertzer, S. Rotter, and H. E. Türeci, Route from spontaneous decay to complex multimode dynamics in cavity QED, Phys. Rev. A **89**, 033820 (2014).

[33] J. Volz, M. Blaha, and A. Rauschenbeutel (unpublished).

[34] P.-O. Guimond, A. Roulet, H. N. Le, and V. Scarani, Rabi oscillation in a quantum cavity: Markovian and non-Markovian dynamics, Phys. Rev. A **93**, 023808 (2016).

[35] S. Mahmoodian, Chiral Light-Matter Interaction Beyond the Rotating-Wave Approximation, Phys. Rev. Lett. **123**, 133603 (2019).

[36] A. S. Prasad, J. Hinney, S. Mahmoodian, K. Hammerer, S. Rind, P. Schneeweiss, A. S. Sørensen, J. Volz, and A. Rauschenbeutel, Correlating photons using the collective nonlinear response of atoms weakly coupled to an optical mode, Nat. Photon. **14**, 719 (2020).

[37] J. Hinney, A. S. Prasad, S. Mahmoodian, K. Hammerer, A. Rauschenbeutel, P. Schneeweiss, J. Volz, and M. Schemmer, Unraveling Two-Photon Entanglement via the Squeezing Spectrum of Light Traveling through Nanofiber-Coupled Atoms, Phys. Rev. Lett. **127**, 123602 (2021).